Journal of Applied Polymer Science

Fluorescent Polymer with CdTe Quantum Dots and 1,8-naphthahmide Fluorescent Polymer: Synthesis, Characterization, and FRET

Weiyun Huang, Lichao Li, Guodong Hui, Deben Chen, Anyong Zhong
College of Chemistry, Sichuan University, Chengdu 610064, China
Correspondence to: A. Zhong (E-mail: zhongany@sina.com.cn)

ABSTRACT: In this paper, we reported a new method to fabricate CdTe quantum dots (CdTe QDs), which were synthesized in aqueous solution using thioglycolic acid and L-phenylalanine (L-Phe) as costabilizing agent. Then, they were transferred into organic phase with the assistance of cetyltrimethylammonium bromide (CTAB) for further utilization. Finally, we use toluene diisocyanate as a bridge between CdTe QDs and polyacrylate (CPA), whose side chain has hydroxyl group, to synthesize a fluorescent composite polymer CdTe-CPA. In addition, we synthesized an organic substance 4-[2,4-di(*tert*-butyl)]phenoxy-*N*-(2-hydroxyethyl)-1,8-naphthalimide (N), and obtained 1,8-naphthahmide fluorescent polymer N-CPA in the same way as it did on CdTe-CPA. The resulting materials were characterized by Fourier transform infrared spectroscopy (FT-IR), gel permeation chromatography (GPC), differential scanning calorimetry (DSC), transmission electron microscope (TEM), and photoluminescence (PL). Then, we studied the fluorescence resonance energy transfer (FRET) between CdTe-CPA and N-CPA. The data obtained from absorption and fluorescence emission spectral indicated that the FRET from N-CPA to CdTe-CPA could be efficiently triggered in the solution of chloroform. © 2012 Wiley Periodicals, Inc. J. Appl. Polym. Sci. 129: 1256–1263, 2013

KEYWORDS: composites; copolymers; synthesis and processing

Received 16 July 2012; accepted 3 November 2012; published online 27 November 2012
DOI: 10.1002/app.38801

INTRODUCTION

CdTe quantum dots (CdTe QDs), as an optical material, have attracted much research attention because CdTe QDs play an important role in imaging and in the manufacture of chemical sensors, optical switches, display devices, and biomedical fluorescent probe.[1–4] However, these studies on CdTe QDs need them have good stability to maintain initial photoluminescence (PL) efficiency, so it is necessary to prevent particle aggregation and agglomeration.[5–8] Polymer has excellent optical characteristics, physical properties, and chemical properties, and significant efforts have been devoted to fabricating the QD-polymer composites[9,10] as incorporating QDs into a polymer matrix is an efficient method to maintain or enhance the PL stability of QDs and on the other hand, to improve their film-forming performance.

Polymer matrices whose side chain could introduce small molecules principally include polycarbonate (PC), polystyrene (PS), polyacrylate (CPA), etc. The aim of this work is to connect amino-group of L-Phe capped on CdTe QDs to the polymer matrix using NCO functional group of toluene diisocyanate (TDI) as the bridge, so there should be an active group in the polymer matrix to react with the other —NCO group of TDI, for instance hydroxyl or amino-group.[11] Cao et al.[12] incorporated CdTe QDs into waterborne polyurethane in aqueous suspension. However, TDI is extremely active in aqueous solution, so the reaction process has to be taken in the organic phase. In this work, polyacrylate (CPA) was synthesized with an active hydroxyl group on the side chain, which can react with the —NCO group of TDI. Thus, the method of using TDI as a bridge to connect CdTe QDs to polymer is feasible.

1,8-naphthalimide derivatives have interesting properties to extend their use as tunable dye lasers, fluorescent molecular switch, fluorescent chemical sensors, and PL thin film.[13] By introducing different electron-donating substituent at the 4-position of 1,8-naphthalimide, their PL emission color can be changed. Based on its excellent fluorescent property, it has been widely used in the fluorescent material field in recent years. Considering that small molecules wrapped in the polymer usually lose its property for their easy escape from the matrix, so chemically binding it to polymer to obtain a fluorescent polymer is an effect way to prevent this phenomenon.

Fluorescence resonance energy transfer (FRET) is a photo-physical process through which the energy transfers from a donor molecule to an acceptor molecule. FRET can be described by the following equation:[14]

$$D* + A \xrightarrow{Kt} D + A*$$

where D* is an excited donor and A is an acceptor molecule at the ground state. *Kt* is the rate constant of energy transfer from donor to acceptor. According to Förster theory, the rate of energy transfer is based on the overlap of emission spectrum of the donor and absorption spectrum of the acceptor, relative orientations of the donor and acceptor transition dipoles, the distance between the donor and acceptor transition dipoles, and PL quantum yield (QY) of the donor.[15,16] The studies in recent years demonstrate that QDs can serve as both donors and acceptors in FRET research field.[17,18] FRET research between dye compounds is also very common,[14] but few papers were devoted to the FRET investigation between polymers. In this case, the understanding of the FRET between these fluorescent polymers would be important for the spectroscopic application.

In this study, we demonstrated a novel method to synthesize fluorescent polymer with CdTe QDs embedded via the chemical bonding between groups of —NH_2 group on the QD surface and —NCO group of TDI, and the other —NCO group of TDI react with hydroxyl group on the side chain of polyacrylate, and employed the same way to synthesize 1,8-naphthahmide contained fluorescent polymer. The optical properties were studied in detail. In our work, we further reported the investigation of the FRET between the two polymers, which may potentially provide theoretical support for the determination of protein structure and the measurement of trace elements. The two fluorescent polymers as-synthesized have excellent stability, which opened new avenues for their widely used.

EXPERIMENTAL

Reagents

Sodium borohydride ($NaBH_4$), thioglycolic acid (TGA), L-phenylalanine (L-Phe), cetyltrimethylammonium bromide (CTAB), petroleum ether (PE), ethyl acetate (EA) azobisisobutyronitrile (AIBN), dibutyltion dilaurate (DBTDL), and TDI were purchased from Chengdu Kelong Chemical and Technology Reagents (Chengdu, China). Tellurium powder, 4-bromo-1,8-naphthalic anhydride, 2-hydroxyethylamine, and 2,4-di(*tert*-butyl)phenol were purchased from Sinopharm Chemical Reagent Co. (Shanghai, China). Methyl methacrylate (MMA), *n*-butyl acrylate (BA), and 2-hydroxyethyl acrylate (HEA) were purchased from Beijing East Chemical Industry Factory (Beijing, China), distilled before use.

All reagents were of AR grade or of the highest purity available.

Synthesis of CdTe QDs

CdTe QDs were synthesized by means of the method reported in the literature with a little modification.[19–22] In brief, 2 mL ultrapure water was added into a mixture of 100.0 mg of $NaBH_4$ and 127.6 mg of tellurium powder in a 25 mL two-necked flask to initiate the generation of NaHTe in an ice bath under nitrogen atmosphere, in which NaHTe dissolved in the supernatant along with the precipitation of white sodium tetraborate at the bottom of the flask. Meanwhile, 456.8 mg of $CdCl_2{\cdot}2.5H_2O$ and 420 μL of TGA were mixed with 200 mL of ultrapure water (deaerated by N_2 for 30 min) in a three-necked flask under stirring, and the pH value of the solution was adjusted to 9–10 with 1 mol L^{-1} NaOH. Then, the freshly prepared NaHTe solution was transferred to the latter mixture under N_2, the mixture was refluxed and stirred vigorously for 2 h to form thiol-stabilized CdTe QDs solution. After that, a certain amount of L-Phe dissolved in ultrapure water and 15 mL of thiol-stabilized CdTe QDs solution were mixed and heated to 96°C and refluxed for 0.5 h under the protection of the N_2. When it cooled to ambient temperature, 328 mg CTAB was added to the system slowly. The precipitate was separated by centrifugation and dried in the vacuum oven; finally, it was dissolved in 10 mL chloroform for further utilization. The product was marked as $^{CTAB/CHCl3}$QDs.

Synthesis of CPA

The procedure was performed in a three-necked flask equipped with a stirrer, a reflux condenser and a constant-pressure dropping funnel. 50 mL anhydrous toluene was added in the flask as solvent; 2.5 mL of MMA, 2 mL of BA, 0.5 mL of HEA, and the initiator (AIBN) were dissolved in 30 mL of anhydrous toluene and slowly added in the system using constant-pressure dropping funnel. The polymerization reaction was performed at 85°C for 5 h to obtain transparent CPA.

Synthesis of CdTe-CPA

A certain amount of CPA dissolved in 20 mL of anhydrous chloroform and 123 μL TDI were added in a three-necked flask which equipped with an economical allihn condenser and a drying pipe, and stirred at 30°C for 3 h. Then, the $^{CTAB/CHCl3}$QDs solution mentioned earlier and 50 μL DBTDL were added to the flask, the mixture was refluxed and stirred at 50°C for 5 h. Orange-yellow product CdTe-CPA was obtained.

Scheme 1 shows the synthetic route of CdTe-CPA, A is L-Phe and TGA stabilized CdTe QDs, B is CPA, C is copolymer, which is synthesis by the reaction of CPA and TDI, and D is the fluorescent polymer CdTe-CPA.

Synthesis of 4-[2,4-di(*tert*-butyl)]phenoxy-*N*-(2-hydroxyethyl)-1,8-naphthalimide (N)

There are two steps for the detailed synthetic routes to the target compounds. First 250 mL aqueous solution with 8 g of 4-bromo-1,8-naphthalic anhydride and 2 g of 2-hydroxyethylamine were added in a 500 mL three-necked flask. The mixture was refluxed and stirred for 5 h, then cooled down and filtered. A khaki 4-bromo-*N*-(2-hydroxyethyl)-1,8-naphthalimide was obtained. Yield: 65.7%. Second, a solution containing 3.41 g (16.6 mmol) of 2,4-di(*tert*-butyl)phenol in 40 mL of anhydrous DMSO was added with 1.65 g (29.5 mmol) of potassium hydroxide. The mixture was stirred at room temperature for 1.5 h under argon atmosphere, then a solution of 5.28 g (16.5 mmol) of 4-bromo-*N*-(2-hydroxyethyl)-1,8-naphthalimide dissolved in 200 mL of dimethyl sulfoxide (DMSO) was added dropwise over 30 min. The mixture was stirred for 8 h at room temperature, neutralized to pH = 7 with 1 mol L^{-1} hydrochloric acid, and then extracted with 20 mL × 3 EA. The organic layer was washed twice with water, dried with anhydrous sodium sulfate. Removal of the solvent under vacuum would result in the crude product, which was purified by column chromatograph (PE/EA = 2/1) to obtain pale yellow solid, followed by recrystallization from EtOH and the yield is 27%.

Applied Polymer SCIENCE

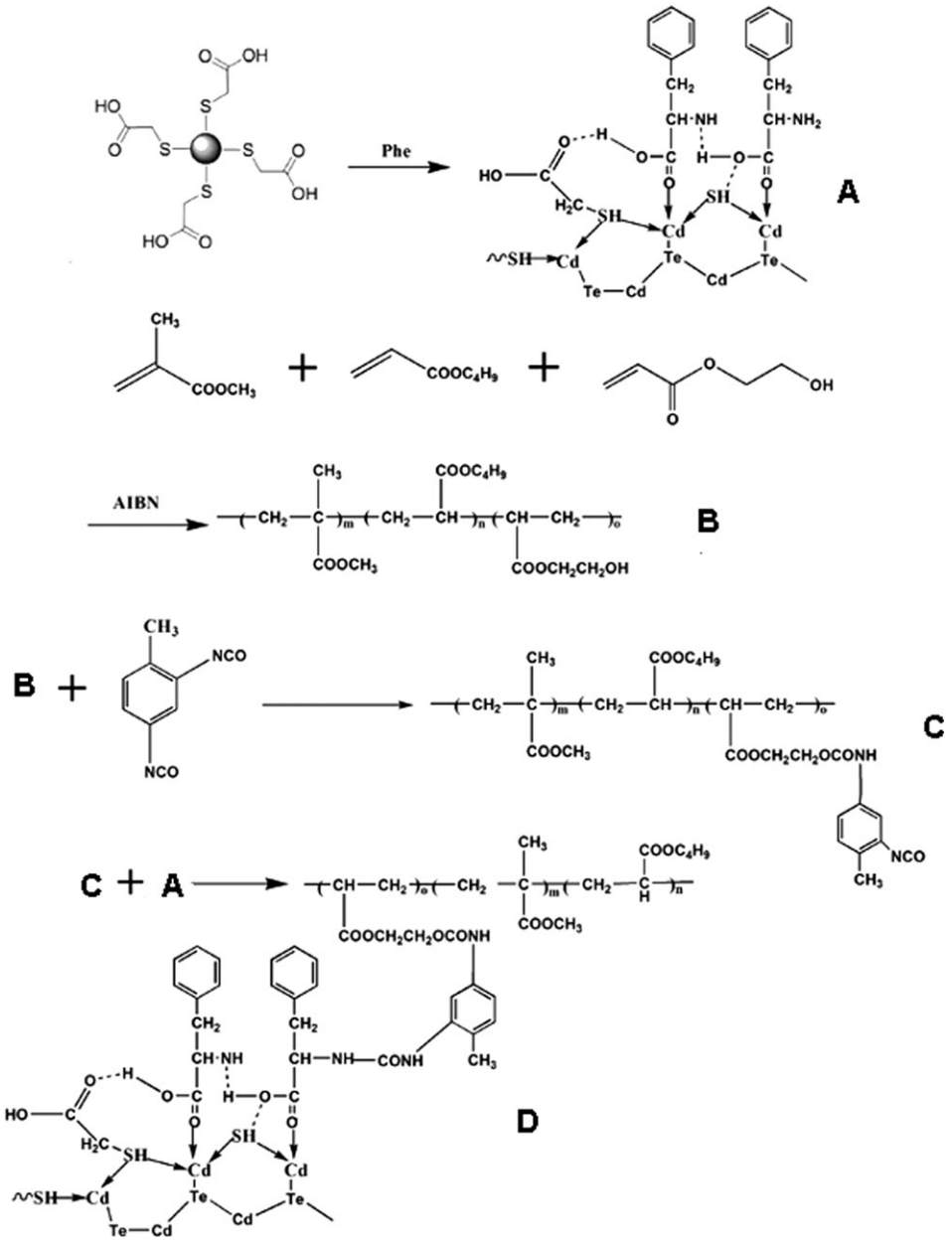

Scheme 1. The synthetic route of CdTe-CPA.

Synthesis of N-CPA

N-CPA was synthesized using the similar procedure as synthesis of CdTe-CPA, using N as starting material. The product is light yellow-green.

Scheme 2 shows the synthetic route of N-CPA, A is 4-bromo-1,8-naphthalic anhydride, B is 4-bromo-*N*-(2-hydroxyethyl)-1, 8-naphthalimide, C is N, D is CPA, E is copolymer which is synthesis by the reaction of CPA and TDI, and F is the fluorescent polymer N-CPA.

FRET between CdTe-CPA and N-CPA

The donor (N-CPA) concentration was 3.5×10^{-4} M and was kept constant for all the experiments whereas acceptor (CdTe-CPA) concentration was variable from 2.5×10^{-4} M to 12.5×10^{-4} M. Placed for 5 min and then measure the PL.

Characterization

The molecular weights and molecular weight distributions are measured by gel permeation chromatography (GPC) with an Agilent HPLC-1100 instrument, while THF is used as the eluent at a flow rate of 1.0 mL min^{-1} at 25°C.

Fourier transform infrared spectra (FTIR) are obtained with an FI-RT670 spectrometer in the wave frequency range of 500–4000 cm^{-1}.

^{1}H-NMR spectra is recorded by a Bruker AVII spectrometer operated at 400 MHz, using tetramethylsilane (TMS) as the internal reference and $CDCl_3$ as the solvent.

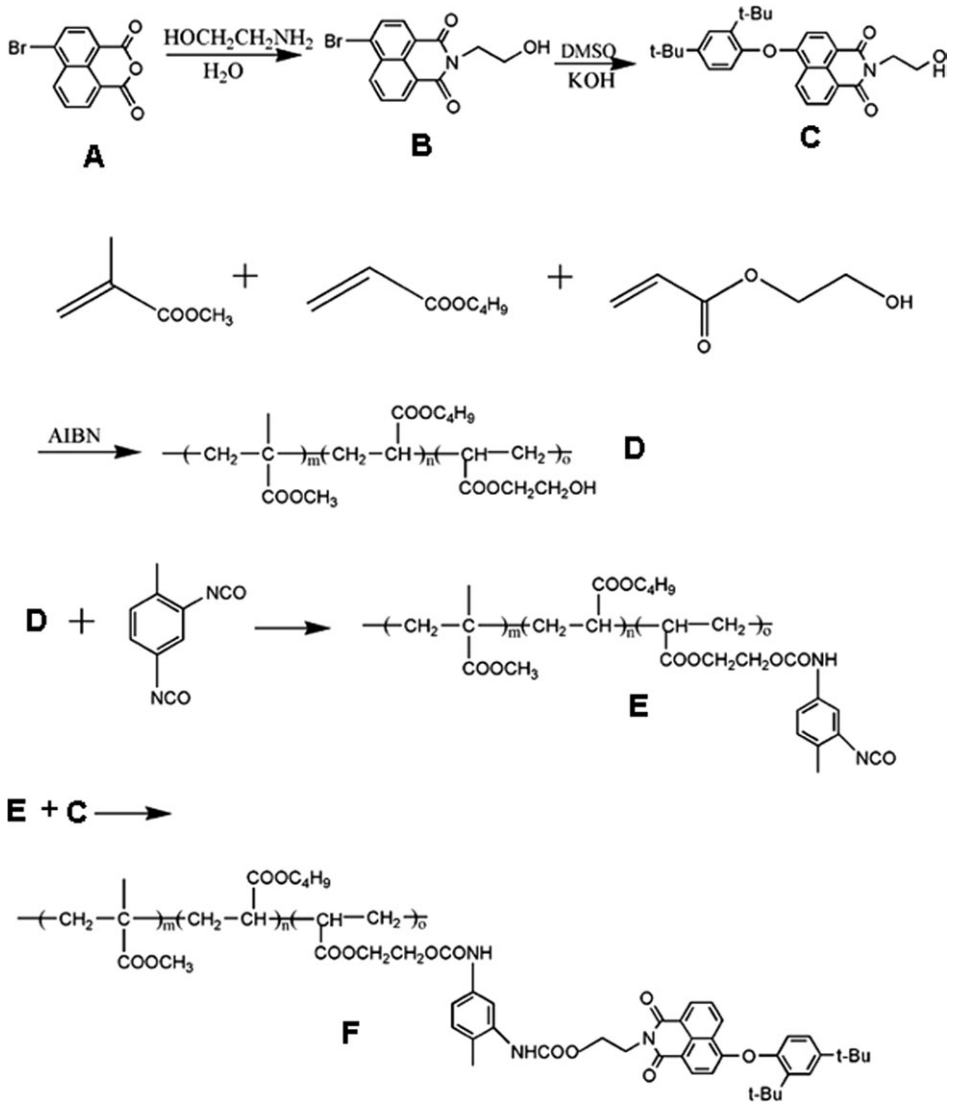

Scheme 2. The synthetic route of N-CPA.

Transmission electron microscopy (TEM) is obtained with a FEI Tecnai G2 F20 FE-TEM measured at high-resolution images.

T_g is obtained by a differential scanning calorimetry (DSC) Q2000 V24.2 Build 107 Calorimeter in the temperature range of 0–300°C, while in the protection of N_2.

The photoluminescence properties are measured using a Hitachi F-7000 fluorescence spectrometer. The PL QYs of CdTe were estimated by using Rhodamine 6G in ethanol as a reference (QY = 95%),[23] and the value of QY was calculated with the following equation:

$$QY_s = \left[\left(A_r L_s n_s^2\right)/\left(A_s L_r n_r^2\right)\right] QY_r$$

Herein, QY_s and QY_r are the absolute QYs of QDs sample and Rohodamine 6G, respectively. A_s and A_r are compared with the absorption value at the excitation wavelength, respectively. n_s and n_r are the refractive index of solvents: $n_{ethanol}$ is 1.359 and n_{water} is 1.333 at room temperature. L_s and L_r are PL integrated intensities of CdTe QDs and Rohodamine 6G excited at 380 nm. The PL QY of CdTe QDs and CdTe-CPA thus are calculated to be 38% and 27%, respectively.

RESULTS AND DISCUSSION

Characterization of CdTe-CPA

Figure 1 shows the typical PL spectra and UV-vis absorption spectrum of L-Phe and TGA capped CdTe QDs in aqueous solution. From the spectra, we can see that the symmetric emission peak located at about 540 nm, which is orange emitted, and the full width at half maximum (FWHM) is about 40 nm. The narrow FWHM and the PL peak reflect the narrow particle size distribution of CdTe QDs. In addition, the absorption spectrum of CdTe QDs is broad, which provides the basic requirement for its application in the energy transfer.

Figure 2 shows the FTIR spectra of CPA (curve a) and CPA+TDI (curve b) and Figure 3 shows the spectra of $^{CTAB/CHCl3}$QDs (curve a), CPA+TDI (curve b), and CdTe-CPA (curve c). From Figure 2, we can see that there is a very obvious peak at 2268 cm^{-1} in

Applied Polymer SCIENCE

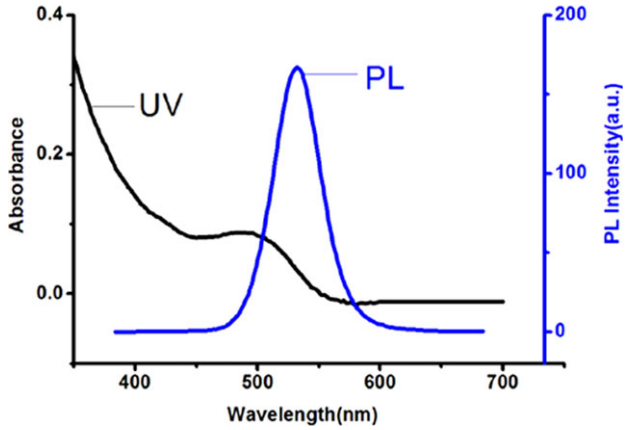

Figure 1. UV spectra and PL spectra of CdTe QDs. [Color figure can be viewed in the online issue, which is available at wileyonlinelibrary.com.]

CPA+TDI compare with CPA, which is the characteristic peak of —NCO group. What's more, there are a triplet peaks between 1250 and 1100 cm^{-1} which belong to NHCOO. The obvious absorption of —OH group occurred at 3325 cm^{-1} in CPA, while the peak was weak in CPA+TDI, implying that —OH groups in CPA reacted with —NCO group of TDI. As shown in Figure 3, the characteristic peak of —NCO groups disappeared in CdTe-CPA, which suggested that —NCO groups had reacted with the $—NH_2$ groups on $^{CTAB/CHCl3}$QDs. In addition, there are the NHCOO characteristic peaks at 1250–1100 cm^{-1} both in CPA+TDI and CdTe-CPA, which confirmed the occurrence of the reaction between —NCO group and reactive $—NH_2$/—OH group. In addition, we could also find the characteristic N—H absorption peaked at 3400–3300 cm^{-1} both in $^{CTAB/CHCl3}$QDs and CdTe-CPA.

Figure 4a shows the relationships between PL intensity and the concentration of CdTe QDs, while Figure 4b shows the relation between PL intensity and the concentration of CdTe-CPA. They both have the same conditions as from a to g the concentration is reduced. From the figure, we can see that they both have the same phenomenon: the PL intensity enhances with the increases of the concentration within a certain range. At higher concentration, the PL intensity begins to decrease. This phenomenon could be explained by the fluorescence quenching mechanism[24–26] originating from the own aggregation when the concentration is relatively large.

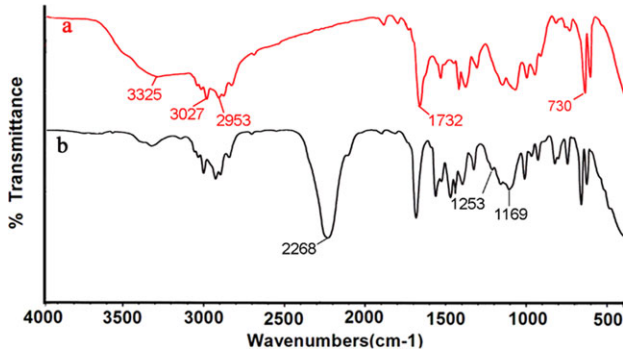

Figure 2. The FTIR spectra of CPA (a) and CPA+TDI (b). [Color figure can be viewed in the online issue, which is available at wileyonlinelibrary.com.]

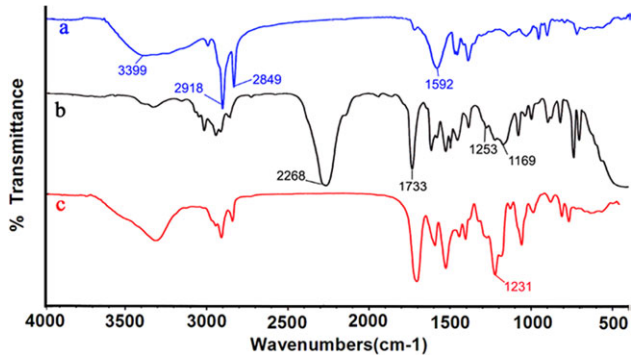

Figure 3. The spectra of $^{CTAB/CHCl3}$QDs (a), CPA+TDI (b), and CdTe-CPA (c). [Color figure can be viewed in the online issue, which is available at wileyonlinelibrary.com.]

Table I shows molecular weight, molecular weight distribution, and glass transition temperature (T_g) of CPA and CdTe-CPA. The results show that M_n and M_w of CdTe-CPA are 6.85×10^3 and 1.82×10^4, while M_n and M_w of CPA are 6.28×10^3 and 1.72×10^4, respectively. Both M_n and M_w of CdTe-CPA are larger than that of CPA due to the existence of the grafted CdTe QDs. This convinced that the CdTe QDs had been successfully introduced onto the main chain of CPA. T_g was determined by

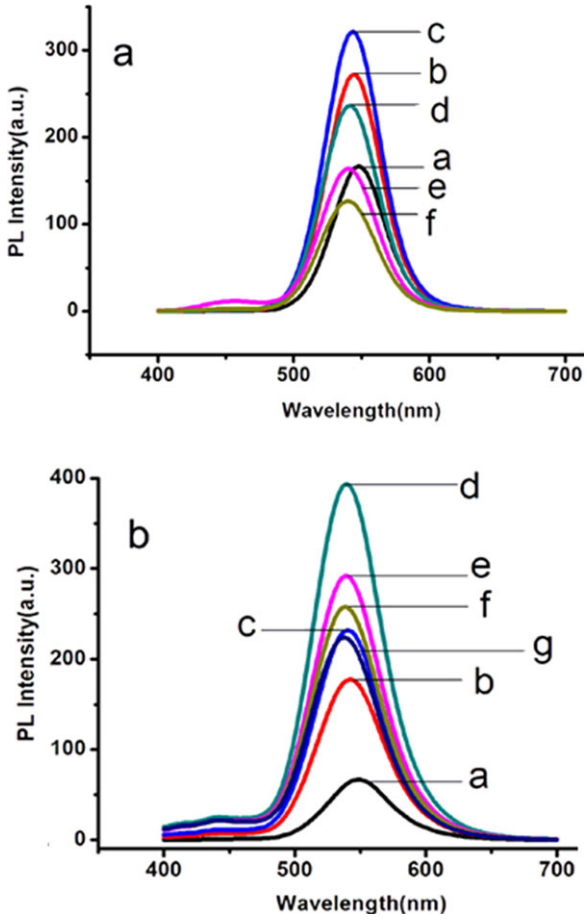

Figure 4. PL of CdTe QDs (a) and CdTe-CPA (b). [Color figure can be viewed in the online issue, which is available at wileyonlinelibrary.com.]

Table I. Molecular Weight, Molecular Weight Distribution and Glass Transition Temperature (T_g) of CPA, CdTe-CPA, and N-CPA

	M_n	M_w	M_w/M_n	T_g (°C)
CPA	6.28×10^3	1.72×10^4	2.73	40.3
CdTe-CPA	6.85×10^3	1.82×10^4	2.66	56.8
N-CPA	7.56×10^3	2.01×10^4	2.66	53.9

DSC and the results showed that T_g of CdTe-CPA reached 56.8°C, much higher than that of CPA (40.3°C), which should be caused by the enhancement of the rigid structure after grafting CdTe QDs on the polymer chain.

Figure 5(a) shows the TEM image of L-Phe and TGA stabilized CdTe QDs, from which we can find that well-dispersed CdTe QDs was gained. The well-resolved lattice fringes for the particle indicate that an excellent crystalline structure of CdTe QDs. The particle size of CdTe QDs is about 5 nm. The TEM image of CdTe-CPA shown in Figure 5(b) demonstrated CdTe QDs were well-dispersed in the CPA matrix with slight aggregation, which indicated a good compatibility between CdTe QDs and CPA. The good compatibility can be ascribed to the strong interaction between the ligand on the CdTe QDs surface and the CPA by forming covalent bonds.

Characterization of N-CPA

Figure 6 shows the ^{1}H-NMR spectra of N, from which we can see there are 12 group peaks. The resonance peaks at 1.38 ppm and 1.39 ppm belong to methyl protons of t-Bu groups (peaks H_1 and H_2), respectively. The methylidyne protons of aromatic ring (peaks H_3, H_4, H_5) were recognized by the signals at 7.59, 7.27, and 7.29 ppm, respectively. The signals at 6.93, 8.48, 8.75, 8.68, and 7.81 ppm belong to methylidyne protons of naphthaline ring (peaks H_6, H_7, H_8, H_9, and H_{10}), respectively. The signals at 3.98 and 4.48 ppm can be attributed to methylene protons (peaks H_{11} and H_{12}), respectively. The signal at 2.52 ppm belongs to protons of hydroxyl group and at 1.63 ppm belongs to solvent peak. From ^{1}H-NMR spectra can conclude that we succeeded in synthesizing N.

Figure 7 shows the FTIR spectra of CPA (curve a), CPA+TDI (curve b), and N-CPA (curve c), from the picture we can find they are similar with the FTIR spectra of CdTe series. Compared with CPA, there is a very obvious peak at 2276 cm^{-1} in CPA+TDI, which can be attributed to the presence of —NCO group. What's more, the characteristic peaks of NHCOO locating at 1250–1100 cm^{-1} suggested that CPA had reacted with one —NCO group of TDI and the other —NCO group is unreacted. In N-CPA, the peak at 2276 cm^{-1} is disappeared, which suggested that —NCO group had reacted. However, the characteristic triplet peaks of NHCOO is not obvious in N-CPA, because these peaks were overlapped with the peaks of N which can be seen from the FTIR spectra of N (curve a) and N-CPA (curve b) shown in Figure 8. Peaks observed at 3422 cm^{-1} and 1655 cm^{-1} can be attributed to acylamino group. Based on these characteristic peaks, we can tell that CPA had reacted with N.

The molecular weight, molecular weight distribution and glass transition temperature (T_g) of CPA and N-CPA show the same phenomenon as CdTe-CPA present in Table I. The M_n and M_w of N-CPA is 7.56×10^3 and 2.01×10^4, while M_n and M_w of CPA is 6.28×10^3 and 1.72×10^4, respectively. Both M_n and M_w are larger than that of CPA due to the grafted N. This convinced the N had already been introduced onto the main chain of CPA. Besides T_g of N-CPA is 53.9°C whereas CPA is 40.3°C, the higher T_g of N-CPA also indicated that rigid N was grafted on the polymer chain.

Effect of FRET

Förster type fluorescence energy transfer depends on the overlap between the donor fluorescence and the acceptor absorption spectra. Figure 9 shows the fluorescence spectra of N-CPA (curve b) and the absorption spectrum of CdTe-CPA (curve a). The overlap of the two spectra is very wide, which facilitate the occurrence of FRET process. The sample was excited at 330 nm as this wavelength can make the fluorescence intensity of donor maximum and acceptor minimum. Figure 10 shows the CdTe-CPA (curve a), N-CPA (curve c), and N-CPA/CdTe-CPA (curve b) fluorescence spectra at the same concentration. When CdTe-CPA was mixed with N-CPA, the fluorescence intensity of N-CPA decreased while CdTe-CPA increased, indicating the energy transfer from N-CPA to CdTe-CPA. From the image we

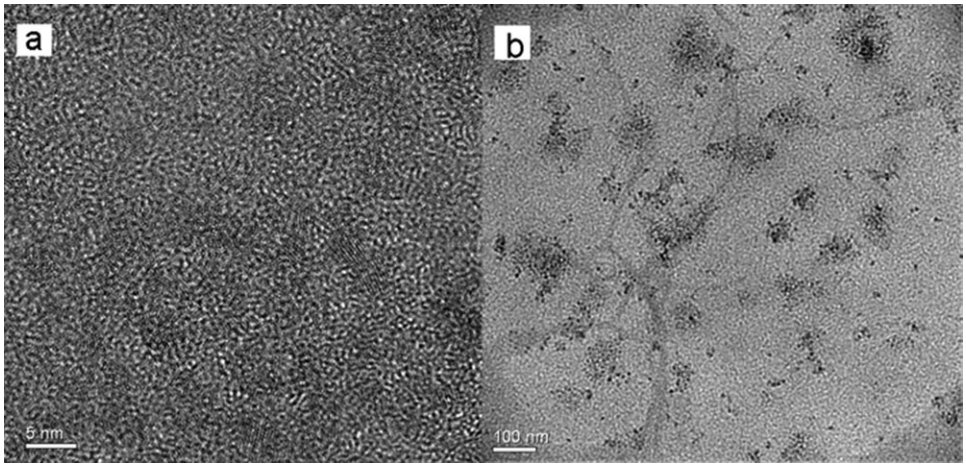

Figure 5. TEM image of CdTe QDs (a) and CdTe-CPA (b).

Applied Polymer SCIENCE

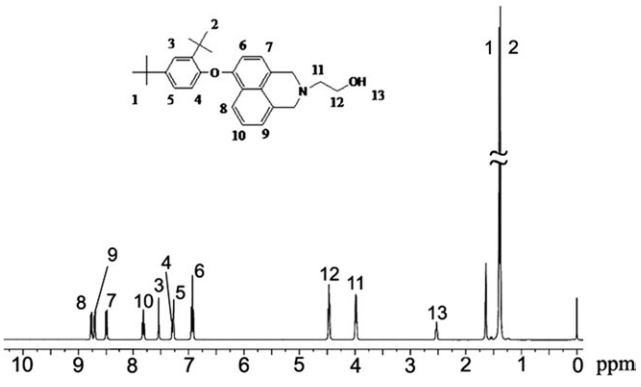

Figure 6. ^{1}H-NMR spectra of N.

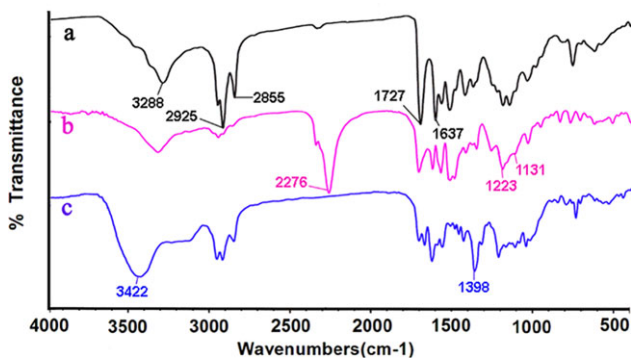

Figure 7. The FTIR spectra of CPA (a), CPA+TDI (b), and N-CPA (c). [Color figure can be viewed in the online issue, which is available at wileyonlinelibrary.com.]

can see, there are characteristic peaks of both CdTe-CPA and N-CPA when the two fluorescent polymers mixed, we can take this advantage to preparation of special anticounterfeit material. Figure 11 shows the fluorescence quenching of N-CPA with increasing CdTe-CPA concentration in chloroform. The concentration of N-CPA was kept constant at 3.5×10^{-4} M for all samples, while increasing the concentration of CdTe-CPA from 2.5×10^{-4} to 12.5×10^{-4} M gradually. The results indicate that with the increase of CdTe-CPA, the fluorescence intensity of N-CPA reduced while the intensity of CdTe-CPA increased, illustrating that FRET occurred between CdTe-CPA and N-CPA.

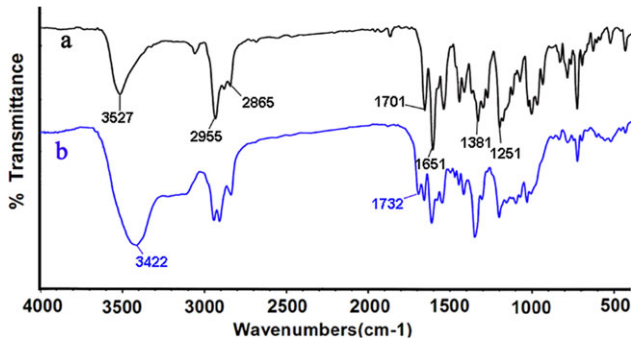

Figure 8. The FTIR spectra of N (a) and N-CPA (b). [Color figure can be viewed in the online issue, which is available at wileyonlinelibrary.com.]

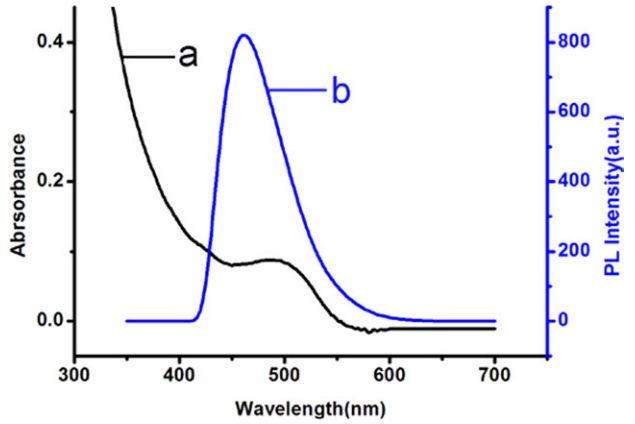

Figure 9. Absorption of CdTe-CPA (a) and fluorescence spectra of N-CPA (b). [Color figure can be viewed in the online issue, which is available at wileyonlinelibrary.com.]

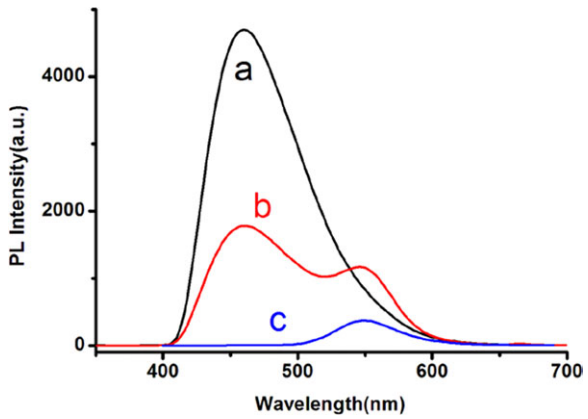

Figure 10. Fluorescence spectra of CdTe-CPA (a), N-CPA (c), and the mixture of CdTe-CPA and N-CPA (b). [Color figure can be viewed in the online issue, which is available at wileyonlinelibrary.com.]

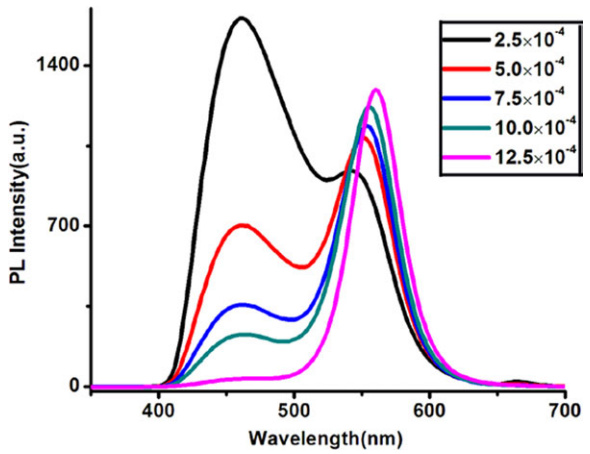

Figure 11. Fluorescence quenching of N-CPA with increasing CdTe-CPA concentration in chloroform. [Color figure can be viewed in the online issue, which is available at wileyonlinelibrary.com.]

In addition, there was a red shift of CdTe-CPA, which is attributed to the self absorption.

CONCLUSIONS

We succeeded in synthesizing CdTe-CPA and N-CPA polymer materials through the chemical grafting method, which had excellent photoluminescence property. In addition we studied the FRET between CdTe-CPA and N-CPA. The PL spectra study showed that the efficient overlap between the emission spectra of donor N-CPA and the absorption spectra of acceptor CdTe-CPA and demonstrated the resonance energy was successfully transferred from N-CPA to CdTe-CPA. Based on the results, this kind of materials may find potential application in measuring of trace elements and the protein research.

ACKNOWLEDGMENTS

These investigations were financially supported by Science and Technological Department of Sichuan Province (No. 2011FZ0107).

REFERENCES

1. Gaponik, N.; Talapin, D. V.; Rogach, A. L.; Hoppe, K.; Shevchenko, E. V.; Kornowski, A.; Eychmuller, A.; Weller, H. *J. Phys. Chem. B* **2002**, *106*, 7177.
2. Poznyak, S. K.; Osipovich, N. P.; Shavel, A.; Talapin, D. V.; Gao, M. Y.; Eychmuller, A.; Gaponik, N. *J. Phys. Chem. B* **2005**, *109*, 1094.
3. Li, P. P.; Liu, S. P.; Yan, S. G.; Fan, X. Q.; He, Y. Q. *Colloids Surf. A* **2011**, *392*, 7.
4. Razykov, T. M.; Ferekides, C. S.; Morel, D.; Stefanakos, E. *Solar Energy* **2011**, *85*, 1580.
5. Cao, Y. W.; Banin, U. *J. Am. Chem. Soc.* **2000**, *122*, 9692.
6. Wang, Y. A.; Li, J. J.; Chen, H.; Peng, X. *J. Am. Chem. Soc.* **2002**, *124*, 2293.
7. Gaponik, N.; Radtchenko, I. L.; Sukhorukov, G. B.; Weller, H.; Rogach, A. L. *Adv. Mater.* **2002**, *14*, 879.
8. Lee, J.; Sundar, V. C.; Heine, J. R.; Bawendi, M. G.; Jensen, K. F. *Adv. Mater.* **2000**, *12*, 1102.
9. Larson, D. R.; Zipfel, W. R.; Williams, R. M.; Clark, S. W.; Bruchez, M. P.; Wise, F. W.; Webb, W. W. *Science* **2003**, *300*, 1434.
10. Wang, M.; Oh, J. K.; Dykstar, T. E.; Lou, X.; Scholes, G. D.; Winnik, M. A. *Macromolecules* **2006**, *39*, 3664.
11. Xu, X. X.; Stöttinger, S.; Battagliarin, G.; Hinze, G. *J. Am. Chem. Soc.* **2011**, *133*, 18062.
12. Cao, X. D.; Li, C. M.; Bao, Q.; Bao, H. F.; Bao, Q. L.; Dong, H. *Chem. Mater.* **2007**, *19*, 3773.
13. Coronado, J. L. Gu; Martin, E.; Montero, L. A.; Fierro, J. L. G.; Garcia de la Vega, J. M. *J. Phys. Chem. A* **2007**, *111*, 9724.
14. Aydin, B. M.; Acar, M.; Arik, M.; Onganer, Y. *Dyes Pigments* **2009**, *81*, 156.
15. Clapp, A. R.; Medintz, I. L.; Uyeda, H. T.; Fisher, B. R.; Goldman, E. R.; Bawendi, M. G.; Mattoussi, H. *J. Am. Chem. Soc.* **2005**, *127*, 18212.
16. Yao, H. Q.; Zhang, Y.; Xiao, F.; Xia, Z. Y.; Rao, J. H. *Angew. Chem. Int. Ed. Engl.* **2007**, *46*, 4346.
17. Lunz, M.; Bradley, A. L.; Chen, W. Y.; Gun'ko, Y. K. *Superlattices Microstruct.* **2010**, *47*, 98.
18. Clapp, A. R.; Medintz, I. L.; Fisher, B. R.; Anderson, G. P.; Mattoussi, H. *J. Am. Chem. Soc.* **2005**, *127*, 1242.
19. Zhang, H.; Lu, G.; Ji, X. L.; Li, Z.; Yang, B. *Chem. J. Chin. Univ.* **2003**, *24*, 178.
20. Li, J.; Yuan, H.; Zhao, K.; Hong, X.; Liu, Y. M.; Ma, L.; Bai, Y. B.; Li, T. *J. Chem. J. Chin. Univ.* **2003**, *24*, 1293.
21. Samanta, A.; Deng, Z. T.; Liu, Y. *Langmuir* **2012**, *28*, 8205.
22. Gao, F.; Lv, C. F.; Han, J. X.; Li, X. Y.; Zhang, J. *J. Phys. Chem. C* **2011**, *115*, 21574.
23. Qu, L.; Peng, X. *J. Am. Chem. Soc.* **2002**, *124*, 2049.
24. Bai, F. L.; Mo, Y. M.; Wang, Z. T.; Chen, D. B.; Li, G. Q.; Hu, H. P. *Polym. Adv. Technol.* **1996**, *7*, 92.
25. Li, G. Q.; Chen, D. B.; Mo, Y. M.; Bai, F. L. *J. Appl. Polym. Sci.* **1996**, *59*, 1463.
26. Li, G. Q.; Chen, D. B.; Bai, F. L.; Mo, Y. M. *J. Polym. Sci. Part B: Polym. Phys.* **1996**, *34*, 1583.